A high capacity polymeric micelle of paclitaxel: Implication of high dose drug therapy to safety and *in vivo* anti-cancer activity

Zhijian He [a, 1], Xiaomeng Wan [a, 1], Anita Schulz [b], Herdis Bludau [b],
Marina A. Dobrovolskaia [c], Stephan T. Stern [c], Stephanie A. Montgomery [d], Hong Yuan [e],
Zibo Li [e], Daria Alakhova [a], Marina Sokolsky [a], David B. Darr [f], Charles M. Perou [f],
Rainer Jordan [b], Robert Luxenhofer [g, *], Alexander V. Kabanov [a, h, **]

[a] Center for Nanotechnology in Drug Delivery and Division of Molecular Pharmaceutics, Eshelman School of Pharmacy, University of North Carolina at Chapel Hill, NC, 27599, USA
[b] Professur für Makromolekulare Chemie, Department Chemie, Technische Universität Dresden, Mommsenstr. 4, 01069, Dresden, Germany
[c] Nanotechnology Characterization Laboratory, Frederick National Laboratory for Cancer Research, Leidos Biomedical Research Inc., Frederick, MD, USA
[d] Department of Pathology and Laboratory Medicine, Lineberger Comprehensive Cancer Center, University of North Carolina at Chapel Hill, Chapel Hill, NC, 27599, USA
[e] Department of Radiology, School of Medicine, University of North Carolina at Chapel Hill, Chapel Hill, NC, 27599, USA
[f] Lineberger Comprehensive Cancer Center, The Animal Study Core, University of North Carolina at Chapel Hill, NC, 27599, USA
[g] Functional Polymer Materials, Chair for Chemical Technology of Materials Synthesis, Julius-Maximilians-Universität Würzburg, Röntgenring 11, 97070, Würzburg, Germany
[h] Laboratory of Chemical Design of Bionanomaterials, Faculty of Chemistry, M.V. Lomonosov Moscow State University, Moscow, 119992, Russia

ARTICLE INFO

ABSTRACT

The poor solubility of paclitaxel (PTX), the commercially most successful anticancer drug, has long been hampering the development of suitable formulations. Here, we present translational evaluation of a nanoformulation of PTX, which is characterized by a facile preparation, extraordinary high drug loading of 50% wt. and PTX solubility of up to 45 g/L, excellent shelf stability and controllable, sub-100 nm size. We observe favorable *in vitro* and *in vivo* safety profiles and a higher maximum tolerated dose compared to clinically approved formulations. Pharmacokinetic analysis reveals that the higher dose administered leads to a higher exposure of the tumor to PTX. As a result, we observed improved therapeutic outcome in orthotopic tumor models including particularly faithful and aggressive "T11" mouse claudin-low breast cancer orthotopic, syngeneic transplants. The promising preclinical data on the presented PTX nanoformulation showcase the need to investigate new excipients and is a robust basis to translate into clinical trials.

1. Introduction

Paclitaxel (PTX) [1] is a powerful antineoplastic agent against metastatic breast cancer, non-small cell lung cancer, advanced ovarian cancer, head and neck cancer and other malignancies [2]. By interfering with tubulin polymerization, thus perturbing microtubule dynamics, PTX leads to chromosome missegregation on multipolar spindles [3]. Apart from excellent potency, PTX is characterized by an extremely low solubility in aqueous media (<1 mg/L) [4], thereby demanding delivery vehicles for parenteral administration. Three formulations are currently clinically approved, two of which by the FDA. Both are blockbusters and make PTX the best selling chemotherapeutic in history [3].

The first clinical formulation of PTX was Taxol. It is characterized by very low drug loading (1% wt.), thus, the amount of the excipient, Cremophor EL/ethanol, necessary to deliver effective doses of PTX is substantial. Excipient plasma concentration can reach 0.4%

* Corresponding author.
** Corresponding author. Center for Nanotechnology in Drug Delivery, UNC Eshelman School of Pharmacy, University of North Carolina at Chapel Hill, Genetic Medicine Building, Room 1094, Campus Box 7362, Chapel Hill, NC, 27599-7362, USA.
E-mail addresses: robert.luxenhofer@uni-wuerzburg.de (R. Luxenhofer), kabanov@email.unc.edu (A.V. Kabanov).
[1] Authors contributed equally to this work.

(v/v) and persist above 0.1% (v/v) for over 24 h [5]. Cremophor EL causes severe allergic, hypersensitivity, anaphylactic reactions and nephro- and neurotoxicity in animals and humans, which significantly limits dosing and requires clinical intervention [6,7].

The clinical demand for alternative formulations led to the development of Abraxane, a nanoparticle formulation (hydrodynamic diameter ≈ 130 nm) comprising human serum albumin and ca. 10% wt. PTX. Evidenced advantages of Abraxane vs. Taxol such as increased antitumor activity and tumor accumulation in several mice xenograft models, significantly higher maximum tolerated doses (MTD) in human, as well as approximately 74% increase of response rates in metastatic breast cancer patients ultimately led to the clinical approval of this new formulation [8]. However, its clinical trials also revealed an increased peripheral neuropathy as compared to Taxol [9]. Moreover, a recent randomized phase III clinical trial of weekly Taxol compared to weekly Abraxane in combination with Bevacizumab as first-line therapy for locally recurrent or metastatic breast cancer indicates that Abraxane offers no benefits to progression-free survival compared to Taxol, while inducing greater hematologic toxicity and sensory neuropathy [10]. Thus, there clearly remains a clinical demand for a formulation of PTX with improved safety profile and therapeutic outcome.

Besides other approaches, polymeric micelles were investigated to formulate PTX [11–13]. For example, Genexol-PM [11], a formulation comprising a block copolymer of poly(ethylene glycol) (PEG) and poly(DL-lactide) (PLA) with 16 wt% PTX is clinically approved in South Korea. NK105, a formulation comprising 23 wt% PTX using a block copolymer of PEG and modified poly(aspartate) undergoes a phase III clinical study [13]. However, even these most advanced formulations only in part overcome the common limitations of PTX formulations. Although the relative PTX content is comparably high, the absolute PTX concentration in the administered solutions is very low for both micellar formulations (Fig. 1). The MTD of Genexol-PM identified as 50 and 60 mg/kg in non-tumor bearing female SPF C3H/HeNcrj mice and nude mice respectively is only 2–3x higher compared to Taxol [11]. NK105 could be safely administered at 100 mg/kg in balb/c female nude mice but only at a rather low concentration (0.12 mg/mL), requiring prolonged intervals of administration [12]. A superior dosage form, which exhibits high drug loading, desirable pharmacokinetics (PK) and tumor accumulation, and low toxicity while increasing therapeutic efficacy, remains elusive.

Here we present preclinical evaluation data on polymeric micelle formulation based on amphiphilic poly(2-oxazoline) (POx) block copolymers with unique polysoap structure [14,15] that has a potential of fulfilling unmet needs in formulation of PTX. This self-assembled nano-sized formulation of PTX is easy to prepare. It exhibits an unparalleled high drug loading of 50% wt., along with excellent shelf stability and controllable sub-100 nm size. In addition, absolute drug concentrations of 45 g/L could be achieved in an injectable formulation. Fig. 1 compares the drug loading and PTX concentrations (maximal and *ad iniectbilia*) and the reported maximal tolerated dose in animal model for the various discussed PTX formulations.

Favorable *in vitro* and *in vivo* safety profiles and a much higher maximum tolerated dose compared to clinically approved formulations were observed. PK analysis revealed higher exposure of the tumor to PTX as compared to Taxol. Subsequently, we observed improved therapeutic outcome in orthotopic tumor models including particularly faithful and aggressive "T11" mouse claudin-low breast cancer orthotopic, syngeneic transplants.

2. Materials and methods

2.1. Materials

Two batches of amphiphilic triblock copolymers P(MeOx$_{33}$-*b*-BuOx$_{26}$-*b*-MeOx$_{45}$), M$_n$ = 10.0 kg/mol, Đ (M$_w$/M$_n$) = 1.14 and P(MeOx$_{47}$-*b*-BuOx$_{21}$-*b*-MeOx$_{36}$), M$_n$ = 9.9 kg/mol, Đ (M$_w$/M$_n$) = 1.19 were synthesized as described in the previous study [14,15]. PTX was purchased from LC Laboratories (Woburn, MA). All other materials were from Fisher Scientific Inc. (Fairlawn, NJ) and all reagents were HPLC grade. The A2780 cells were originally obtained from Sigma-Aldrich. Cells were cultured in DMEM medium (Gibco 11965-092) supplemented with 10% FBS and 1% pen-strep.

2.2. Methods

2.2.1. Preparation of POx/PTX polymeric micelles

POx/PTX micelles were prepared by a thin film method (Fig. S1 and S2). Briefly, pre-determined amounts of POx and PTX (stock solution 10–20 g/L in ethanol) were dissolved in ethanol (5–10 g/L) and mixed, followed by complete removal of volatiles. We tested and optimized small (1–5 mg scale, air flow at 40 °C) and large scale (200 mg scale, rotary evaporator) production methods to control the thin film formation process (Fig. S1 and S2). Appropriate amounts of deionized (DI) water or normal saline were used to rehydrate the dried thin-film under heating at 50–60 °C for up to 20 min in order to obtain drug loaded polymeric micelles. The resulting micelle formulation was stored as aqueous solution in refrigerator for up to 2 weeks or as lyophilized powder.

The drug concentrations in POx micelles were measured by reverse-phase HPLC method with a Nucleosil C18 − 5μ column (250 mm × 4.6 mm) in an Agilent 1200 HPLC equipment. Each sample was diluted 20 times in mobile phase (ACN/water; 55/45, v/v) and 20 μL diluted sample was injected into the HPLC. The retention times of PTX was approximately 5.0 min and detection wavelength was 227 nm while the flow rate was 1.0 mL/min and column temperature was 30 °C. A standard curve range from 5 μg/mL to 200 μg/mL was used to calibrate the quantity of PTX.

The drug loading capacity (LC), loading efficiency (LE) and drug loading (DL) were calculated using following equations (a)–(b):
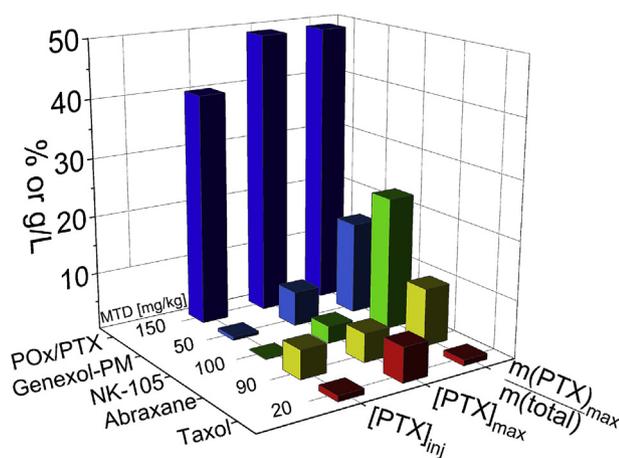
Fig. 1. Comparison of various clinically approved paclitaxel (PTX) formulations. PTX formulations in clinical trials and the POx/PTX formulation discussed in the present contribution. While Abraxane and Taxol are clinically approved by FDA, NK105 and Genexol-PM are currently being investigated in clinical trials. Taxol contains only about 1%wt. of active ingredient (m(PTX)$_{max}$/m(total)), while Genexol-PM and NK105 have a much higher loading capacity. The maximal paclitaxel concentration in solution (PTX$_{max}$) achieved with all four formulations is below 10 g/L, while POx/PTX can reach almost 50 g/L. Compared to Abraxane and POx-PTX, NK105 and Genexol-PM formulations are significantly diluted down for injection, so that final PTX concentrations ([PTX]$_{inj}$) are well below 1 g/L [11,12]. Of all compared PTX formulations, the novel POx/PTX formulation exhibits the highest maximum tolerated dose (MTD) in mice.

where M_{drug} and $M_{excipient}$ are the weight amounts of the loaded (solubilized) drug and polymer excipient in the dispersion, while $M_{drug\ added}$ is the weight amount of the drug initially added to the dispersion.

$$LC = M_{drug}/\left(M_{drug} + M_{excipient}\right) \cdot 100\%, \qquad (a)$$

$$LE = M_{drug}/\left(M_{drug\ added}\right) \cdot 100\%, \qquad (b)$$

A Nano-ZS (Malvern Instruments Inc., UK) DLS equipment was used to measure size distribution of POx micelles. Briefly, each sample was diluted 50 times with DI H_2O or 10 mM NaCl to yield 1 g/L final polymer concentration before the measurement. The hydrodynamic diameters of POx/PTX micelles was determined by intensity-mean z-averaged particle size (effective diameter) and the polydispersity index (PDI) from cumulant analysis. Results were obtained from the average of three independent micelle samples.

The morphology of POx/PTX micelles was studied using a LEO EM910 TEM operating at 80 kV (Carl Zeiss SMT Inc., Peabody, MA). Digital images were obtained using a Gatan Orius SC1000 CCD Digital Camera in combination with Digital Micrograph 3.11.0 software (Gatan Inc., Pleasanton, CA). One drop of each diluted POx/PTX micelle solution (dilute 500 or 1000 times using DI H2O) was deposited on a copper grid/carbon film for 5 min and excess solution was wicked off using fine filter paper. Then one drop of staining solution (1% uranyl acetate) was added and allow to contact for 10 s prior to the TEM imaging.

The drug release studies for POx/PTX micelles were performed using membrane dialysis method against phosphate buffered saline (PBS, pH 7.4) at 37 °C. Briefly, POx/PTX micelles were diluted in PBS to achieve approximately 100 μg/mL of PTX final concentration. Subsequently, 100 μL of the diluted micelle solutions were added into floatable Slide-A-Lyzer MINI dialysis devices (100 μL capacity, 3.5 kDa MWCO; Thermo Scientific) and suspended in 20 mL PBS in compliance with the sink conditions. Three devices were used for every time point. At each time point the samples were withdrawn from dialysis device and quantified by HPLC to obtain remaining drug amount of sample. Drug release profiles were constructed by plotting the amount of PTX drug released from POx/PTX micelles over time.

2.2.2. In vitro complement activation, hemolysis, blood coagulation and cytotoxicity

These studies were carried out following the protocols established and published by the Nanotechnology Characterization laboratory (http://ncl.cancer.gov/working_assay-cascade.asp).

2.2.3. Serum albumin quenching studies

Fluorescence emission spectra were obtained using a Pelkin-nElmer LS 55 Fluorescence spectrometer equipped with a thermostatted cell holder, a Xenon Flash lamp, a Monk-Gillieson type monochromator, and a variable slit system. Emission spectra were recorded in phosphate buffered saline (PBS: 140 mM NaCl, 1.9 mM NaH_2PO_4, 8.1 mM Na_2HPO_4, pH 7.4) from 300 to 440 nm (data shown up to 410 nm) after excitation at 295 nm. Both excitation and emission slits were set at 10 nm. BSA stock solution of 2.5 μM was freshly prepared by dissolving bovine serum albumin in 150 mM PBS. To ensure proper mixing all samples were gently mixed by using a laboratory vortex. The samples were then incubated for 30 min at 25 °C before measuring the fluorescence. Fluorescence emission spectra of tryptophan residues were measured at different sample concentrations. Presented data represents average of triplicate samples.

2.2.4. Serum binding studies

Reverse-phase Thermo Scientific™ SOLA™ HRP solid phase extraction (SPE) cartridges were used for separation and determination of micellar (encapsulated) and non-micellar (free) paclitaxel (PTX) in serum based upon the selective retention of micellar (encapsulated) PTX and non-micellar (protein bound) PTX on the cartridge. The former exhibited no retention, while the latter was retained on the stationary phase and eluted only with acidified methanol.

Sample preparation was performed as follows. The formulations and PTX solutions (100 μL POx/PTX 50/40, 50/20, 50/10, Taxol and free PTX (dissolved in small amount of EtOH) comprising ^{3}H-labeled PTX (2.5 μCi/mg PTX) were added to 2 mL of fetal bovine serum (FBS), incubated at 37 °C, and 200 μL samples were collected from the mixture solution after 1h and 4h. Each 200 μL serum sample was added to 200 μL of POx solution (2 g/L) in phosphate buffered saline, pH 7.4.

To separate micellar and non-micellar (free) paclitaxel the following procedure was used:

(A1) Column conditioning: Add 0.5 mL methanol (to waste)
(A2) Equilibrate: Add 0.5 mL water (to waste)
For the next steps, collect the effluent of A3 and A4 as this contains the micellar paclitaxel fraction. This fraction requires further clean up, described below.
(A3) Application: load pre-treated sample (collect)
(A4) Wash 1: 2 × 0.25 mL POx in phosphate buffered saline (2 mg/mL), pH 7.4 added sequentially (collect)
(A5) Wash 2: 2 × 1 mL water/methanol (90:10 v/v) added sequentially (to waste)
(A6) Elution: 0.5 mL methanol + 0.1% formic acid (collect)

2.2.5. In vivo studies

All animal procedures were performed in compliance with United States federal animal welfare regulations, and protocols were approved by the Institutional Animal Care and Use Committee. All animals used in PK, biodistribution, MTD, toxicology and efficacy studies were allowed to acclimate for at least 72 h in the animal facilities before experiments. Animals were exposed to a 12 h light/dark cycle and received food and water ad libitum throughout the studies. Dosages of POx/PTX micelle formulations or commercial drugs Taxol and Abraxane are expressed as the quantity of PTX administered.

2.2.6. MTD studies

MTDs for Taxol, Abraxane and POx/PTX micelles were determined in a dose escalation method in female nude mice (tumor-free 6–8 weeks of age). Animals (n = 3 per group) received i.v. injections of POx/PTX micelles (20, 40, 60, 90, 120, 150, 175 and 200 mg/kg), Taxol (20, 25, and 30 mg/kg), Abraxane (30, 60, 90 and 120 mg/kg), and saline as a control (q4d × 4). Mice survival and changes in body weight were observed daily over two weeks in all groups. The highest dose that did not cause toxicity (as defined by a median body weight loss of 15% of the control or abnormal behavior including hunched posture and rough coat) was defined as MTD. Changes in histopathology such as inflammation, or presence of necrotic cells were used to assess cytotoxicity occurring after treatment.

2.2.7. Toxicology studies

Healthy Balb/c mice received POx alone, POx/PTX and Taxol at MTD dose. The following day mice were sacrificed and blood were withdrawn and a comprehensive blood chemistry panel were performed. Major organs including heart, liver, kidney, spleen, lung

and brain were harvest, fixed in formalin, and subjected to pathological analysis by H&E staining. In addition, tumor bearing animals were sacrificed two weeks post fourth injection and organs were harvested according to the same procedures as healthy mice.

2.2.8. PK and biodistribution studies

2.2.8.1. Tumor-free mice. Female Balb/c mice (6—8 weeks of age) were administered a single dose of Taxol (20 mg/kg) or POx/PTX micelles (150 mg/kg) containing ^{3}H-labeled PTX (5 µCi/mouse) via tail vein. At various sampling times (0.083, 0.5, 1, 2, 6, 24, 72, and 168 h post) a group of animals (n = 3) were euthanized and blood collected from cardiac puncture was analyzed for PTX plasma concentration by measuring radioactivity. The tissues (brain, lung, kidney, spleen, liver, and heart) were also removed, washed in ice-cold saline, weighted and homogenized in a glass tissue homogenizer (Tearor™, BioSpec Products, Inc.), followed by radioactivity level determination using a Tricarb 4000 (Packard, Meriden) to quantify tissue distribution.

2.2.8.2. Tumor-bearing mice. Female nude mice (6—8 weeks of age) were implanted with 8×10^6 A2780 ovarian cancer cells in 50% growth medium and 50% Matrigel (BD Biosciences) by subcutaneous injection. When tumors were about 200 mm^3 volume, mice were randomized (n = 4 per group) such that the mean tumor weights were similar between groups. Mice were then administered a single dose of above-mentioned formulations. At various time points, blood and tissue samples were obtained accordingly.

2.2.9. Efficacy and POx/PTX tumor accumulation studies

2.2.9.1. A2780 ovarian cancer xenograft model. Female athymic nude mice (6—8 weeks) were subcutaneously inoculated in the right flank with 8×10^6 human A2780 ovarian cancer cells (Sigma Aldrich) resuspended in 50% growth medium and 50% Matrigel. Two sets of experiments were performed: early stage tumor treatment starting after tumor sizes reached ca. 100—200 mm^3; or late stage tumor treatment when tumor sizes reached ca. 400 mm^3. Animals were randomized into groups of seven mice such that the mean tumor volumes were similar between groups and then administered with following formulations: 1) Normal saline; 2) Taxol (20 mg/kg PTX at determined MTD dose); 3) Abraxane (45 and 90 mg/kg PTX at determined ½MTD and MTD doses); 4) PTX loaded micelles (75 and 150 mg/kg at determined ½MTD and MTD doses). The formulations were administered via tail vein following q4d × 4 regimen (on the days 0, 4, 8, 12). Tumor growth was monitored twice weekly for 15 weeks or earlier end-points defined by tumor volume (>2000 mm^3), animal weight loss (>15%), or animals becoming moribund. Tumor length (L), width (W) were measured and tumor volume (TV) was calculated as TV = 1/2 × L × W^2. Survival and body weight were monitored daily. Tumors were removed at the end of the observation and subjected to histopathological examination.

2.2.9.2. Orthotopic model of LCC6-MDR human TNBC. The LCC6-MDR cells (obtained from Dr. R. Clarke, Georgetown University Medical School, Washington DC) expressing high levels of *P*-glycoprotein (P-gp) were originated from LCC6-WT cells stably transfected with a retrovirus vectored mdr1 gene. The parent LCC6-WT cells were derived from estrogen receptor (ER)-negative, aggressive and metastatic MDA-MB-435 cells. The orthotopic model was obtained by directly transplanting LCC6-MDR cells into mice mammary fat pad (5 million cells/mouse).

2.2.9.3. T11 orthotopic, syngeneic transplant (OST) cancer model. T11 model mice are assessed using described practices of the Mouse Phase 1 Unit (MP1U) of UNC (*e.g.*, tumor regression, large

cohort size, *etc.*). When tumors were noted to be approximately 10—50 mm^3 in size, animals were treated as described and tumor response was assessed by weekly caliper measurements. Data in Fig. 8 are averaged data, with volumes calculated using previously mentioned formula. Tumor-bearing mice were euthanized at the indicated times for morbidity, tumor ulceration, or tumor volume more than 3000 mm^3.

2.2.10. PK and data analysis

PK parameters were assessed with Phoenix WinNonlin (version 6.0) using non-compartmental analysis. Statistical comparison of efficacy and tumor accumulation data is one-way ANOVA with Holm-Sidak post-hoc test for multiple comparisons at a significance level of p < 0.01 (Graphpad Prism, version 5.1.). If groups fail the normality or equal variance test, ANOVA on ranks with the Tukey post-hoc test were used for multiple comparisons.

3. Results

3.1. Characterization of PTX-loaded POx micelles

The POx/PTX formulation was prepared by a very simple, robust and highly reproducible thin film hydration method [14—16] (Fig. 2A and B, Supplementary Fig. S1 and S2). POx/PTX micelles (<100 nm effective diameter) with drug loading of approx. 50 wt% spontaneously self-assemble during rehydration of the dry film (Fig. 2B, Table S1) [16]. In this work, we concentrated on two formulations, comprising 50 g/L excipient and 40 or 20 g/L PTX, subsequently termed POx/PTX 50/40 and POx/PTX 50/20, respectively. As opposed to Abraxane, the micelle formulations are almost clear solutions with micelles of about 20—80 nm effective diameter and a narrow size distribution (Fig. 2C and D). These solutions are directly lyophilizable and redispersed in desired aqueous buffer, exhibit a neutral ζ-potential and excellent stability (Fig. S3—5; Table S2). In addition, these formulations can be directly injected due to their low viscosity.

3.2. Serum binding studies

Micelles are dynamic structures that can exchange both the surfactant and the drug with the surroundings. Partitioning of the PTX from the micelles to the aqueous media should be very low due to low drug solubility (approx. 1 mg/L). However, in the blood the drug can bind with the serum proteins. Therefore, we studied interaction of POx/PTX with the bovine serum albumin (BSA) by determining the quenching of the fluorescence of albumin tryptophan [17]. While the polymer alone had little effect on the BSA tryptophan fluorescence, the POx/PTX formulation produced a marked fluorescence quenching, which was increased as the drug concentration increased (Fig. S6). Importantly, the fluorescence quenching was more pronounced at a higher POx/PTX ratio.

Therefore, the distribution of the drug between the micelles and serum was assessed using a solid phase extraction (SPE) column (SOLA™ HRP) that binds protein-bound and unbound drug, but not the micelles. First, we demonstrated that in the absence of serum most of the drug (~83—88%) applied to the column in POx/PTX eluted in the micelle fraction (Table S3). The size of the particles in this fraction was 50 nm by DLS, corroborating the presence of intact drug loaded micelles. Only ~9—15% PTX were retained in the column and subsequently extracted by the acid-methanol wash. On the contrary, when plain PTX was loaded onto the columns, the paclitaxel was almost exclusively found in the fraction corresponding to the acid-methanol wash (Table S4). Next, various POx/PTX formulations were mixed at different ratios with 2 mL of the fetal bovine serum (FBS) to mimic the conditions that may realize
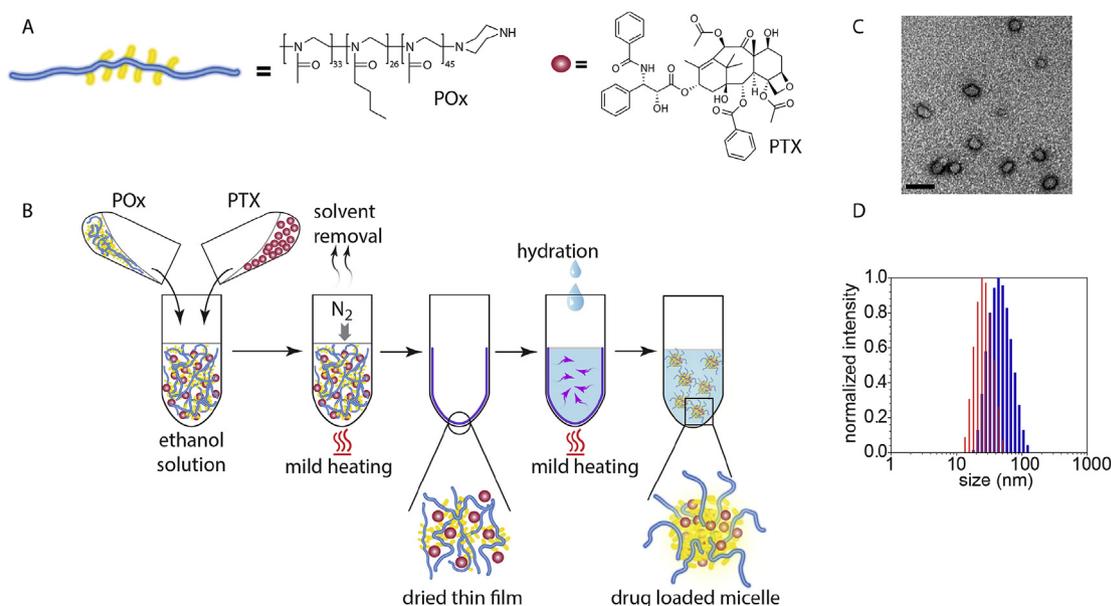
Fig. 2. Construction and physicochemical properties of PTX nanoformulations. (**A**) Schematic and chemical structures of poly(2-oxazoline) triblock copolymer and PTX. (**B**) The nanoformulation is easily prepared employing the thin-film approach. (**C**) Transmission electron microscopy (TEM) shows the spherical morphology of the nanoformulation. (Scale bar = 100 nm) (**D**) Small size and narrow size distribution is corroborated by dynamic light scattering (DLS) (blue: POx/PTX 50/40 g/L, red: POx/PTX 50/20 g/L). (For interpretation of the references to color in this figure legend, the reader is referred to the web version of this article.)

upon injection of the drug in the blood and incubated for either 1 h or 4 h before the column separation (Table 1). In this case at the lower drug concentration ([PTX] = 0.27 mg/mL that correspond to 20 mg/kg PTX dose in the animal studies) only ~62% of PTX eluted with the micelles while the rest was bound to the column and was only partially recovered. As the drug (and polymer) concentration increased ([PTX] = 2 mg/mL, similar to 150 mg/kg PTX in the animal studies) the portion of the drug in the micellar fraction (as well as the overall drug recovery) was also increased markedly to > 80%. In contrast, only about 20% of PTX in Taxol formulation was eluted in the micellar fraction. Free PTX, without excipient, was found to bind to serum proteins almost quantitatively.

3.3. MTD and toxicology profiles of POx/PTX in nude or healthy mice

We investigated MTD by dose escalation in NCI-Nu/Nu mice in a regimen of every fourth day for a total of 4 injections (q4d × 4), which was also employed in subsequent antitumor efficacy studies. For the clinically approved formulations our studies confirmed MTDs reported in the literature (20 mg/kg for Taxol and 90 mg/kg for Abraxane).

It should be noted that we removed endotoxins by heating POx to 200 °C for 24 h (Fig. 3). We also confirmed the low complement activation previously observed for POx/PTX [14] using an alternative protocol (Nanotechnology Characterization Laboratory protocol NCL ITA-5). Similar to the negative control, the POx polymer itself and POx/PTX do not activate complement at ≤ 1.5 mg/mL, being the 2-fold concentration of POx/PTX we would expect in animal or patient's serum after injection even considering a 7-fold increased PTX dose administered compared to Taxol. In contrast, Taxol at 1.5 mg/mL (a clinically relevant positive control) revealed strong complement activation (Fig. 3A) [14]. POx and POx/PTX formulation are not hemolytic and do not induce platelet aggregation (Fig. 3B,C). Interestingly, we found evidence that POx and POx/PTX formulations can result in prolonged activated partial thromboplastin time (APTT) without affecting the thrombin or prothrombin time (PT) (Fig. 3D–F). Such retardation of coagulation could be beneficial to breast cancer patients as it was demonstrated that haemostatic alterations and pro-coagulant systems, especially the formation of venous thromboembolism (VTE), are frequently observed complications following chemotherapy [18]. In vitro cytotoxicity of PTX/POx in hepatic and kidney cells was similar to that of Abraxane (Fig. S8-9 and Table S5).

Table 1
SPE column separation of serum samples incubated with POx/PTX 50/40, POx/PTX 50/20, or Taxol and free PTX for 1 h and 4 h.

Formulation	Concentration (g/L)		PTX elution, %			
			1 h incubation[a]		4 h incubation	
	PTX	POx	Non-protein bound[b]	Protein bound[c]	Non-protein bound[b]	Protein bound[c]
POx/PTX 50/40	0.27	0.33	62.0 ± 2.9%	33.9 ± 0.4%	52%	27%
POx/PTX 50/40	2.0	2.5	84.1 ± 1.5%	14.2 ± 0.5%	74%	16%
POx/PTX 50/20	2.0	5.0	81.8 ± 1.8%	15.6 ± 2.1%	68%	15%
POx/PTX 50/10	2.0	10	80.8 ± 0.6%	15.1 ± 1.9%	70%	16%
Taxol	0.27	0	20.3 ± 1.9%	74.6 ± 4.3%	7%	46%
PTX	0.27	0	1.4 ± 0.1%	90.4 ± 0.2%	1%	94%

[a] Data represents means ± SD (n = 3).
[b] Fractions A3 and A4 as described in the experimental section.
[c] Fractions A6 as described in the experimental section.
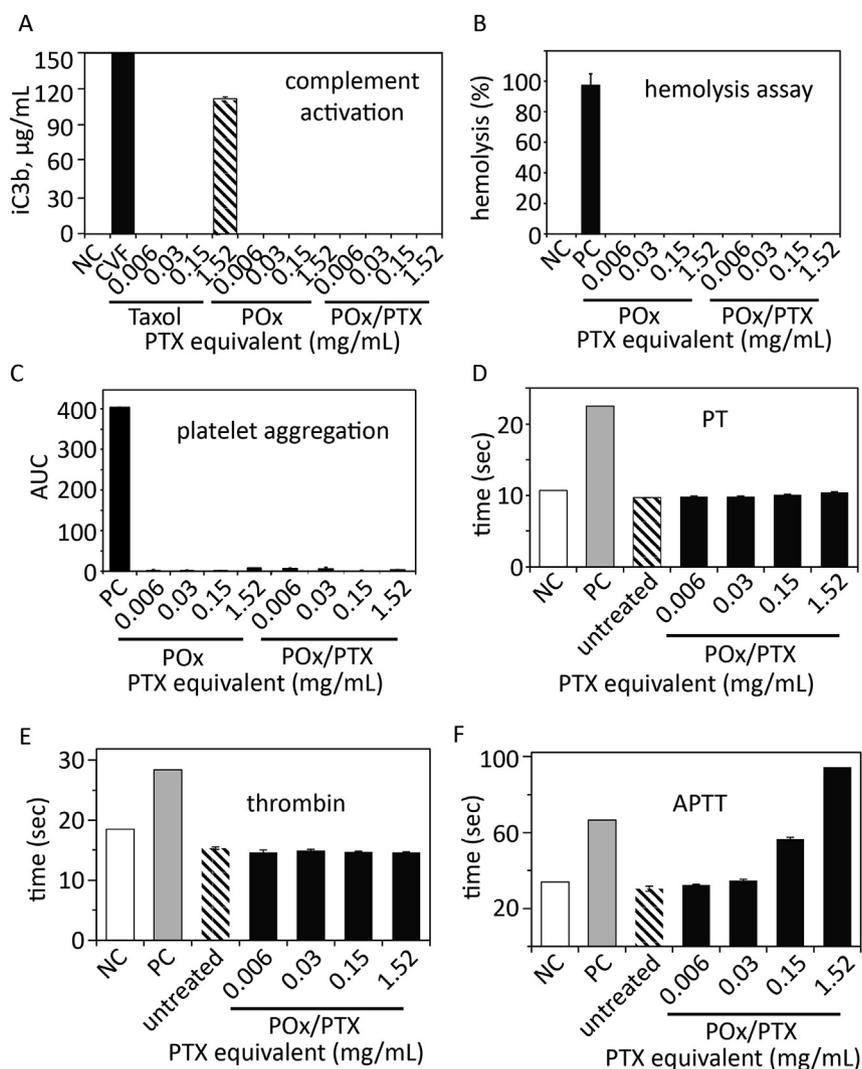
Fig. 3. In vitro toxicity evaluation. (A) Complement activation, (B) hemolysis, (C) platelet aggregation, (D) prothrombin time (PT), (E) thrombin time and (F) activated partial thromboplastin time (APTT) of POx polymer or POx/PTX micelles (concentration range from 0.006 to 1.52 mg/mL, 1.52 mg/mL corresponds to approx. 2 fold the maximum value we would expect to observe in humans after injection and distribution) as compared to Taxol. Negative control (NC) was PBS (complement activation, hemolysis) and normal plasma standard (PT, thrombin and APTT), respectively. As positive control, cobra venom factor (CVF, complement activation), Triton X-100 (hemolysis), collagen (platelet aggregation) and abnormal plasma standard (PT, thrombin and APTT) were used, respectively. Data are shown as means ± SD (n = 3 or n = 2 for C).

POx/PTX treated mice barely showed weight loss and no noticeable changes in behavior up to 150 mg/kg dose (Fig. 4A). In clinic, cumulative peripheral neuropathy represents a major side effect affecting patient's quality of life. Although a detailed study of this issue was outside the scope of the present work, we would like to note that animals that received POx/PTX showed less symptoms of peripheral neuropathy, such as a hunched back, both at the same dose and at MTD as compared to animals treated with Abraxane or Taxol. We found that mice administered four times with 175 mg/kg micelles lost over 15% body weight. However, a single injection of 200 mg/kg of POx/PTX micelles was well tolerated without obvious sign of toxicity. We also tested POx polymer alone at equivalent and higher dose (187.5 mg/kg − 500 mg/kg), and no remarkable changes in general activity and body weight were observed, showing that relatively high doses of the vehicle are well tolerated after repeated injection in vivo (Table S6).

Thus, the MTD for POx/PTX micelles determined under q4d × 4 regimen was 150 mg/kg, i.e. more than seven fold as high as that of Taxol (20 mg/kg) and significantly higher than that of Abraxane (90 mg/kg) (Fig. 4B). Although it is not straightforward to compare

MTD in mice or other animals to that in human, the relative MTDs of Taxol, Genexol-PM, Abraxane and NK105 correlated reasonably well with human MTD or recommended doses for these formulations [19—21]. Therefore, it is reasonable to assume that the present nanoformulation could increase MTD also in humans above current possibilities.

In vivo, safety of POx/PTX was also evaluated in Balb/c by examining clinical chemistry parameters for kidney and liver function. There were no significant changes for blood urea nitrogen (BUN), alanine amino transferase (ALT), albumin values and other blood chemistry parameters with the exception of a slightly increased blood glucose levels for the POx/PTX group. Histopathology of major organs of animals two week after four injections (q4d × 4) at MTD dose (Fig. 4C and Table S7) was performed in nude mice.

Histology reported no toxicity to lung, spleen, brain, and heart for all formulations tested. Mild toxic degenerative changes of centrilobular hepatocyte atrophy were evident in samples from animals exposed to Abraxane and Taxol (Fig. 4C, solid arrow in liver samples). This was also observed in POx and POx/PTX samples,
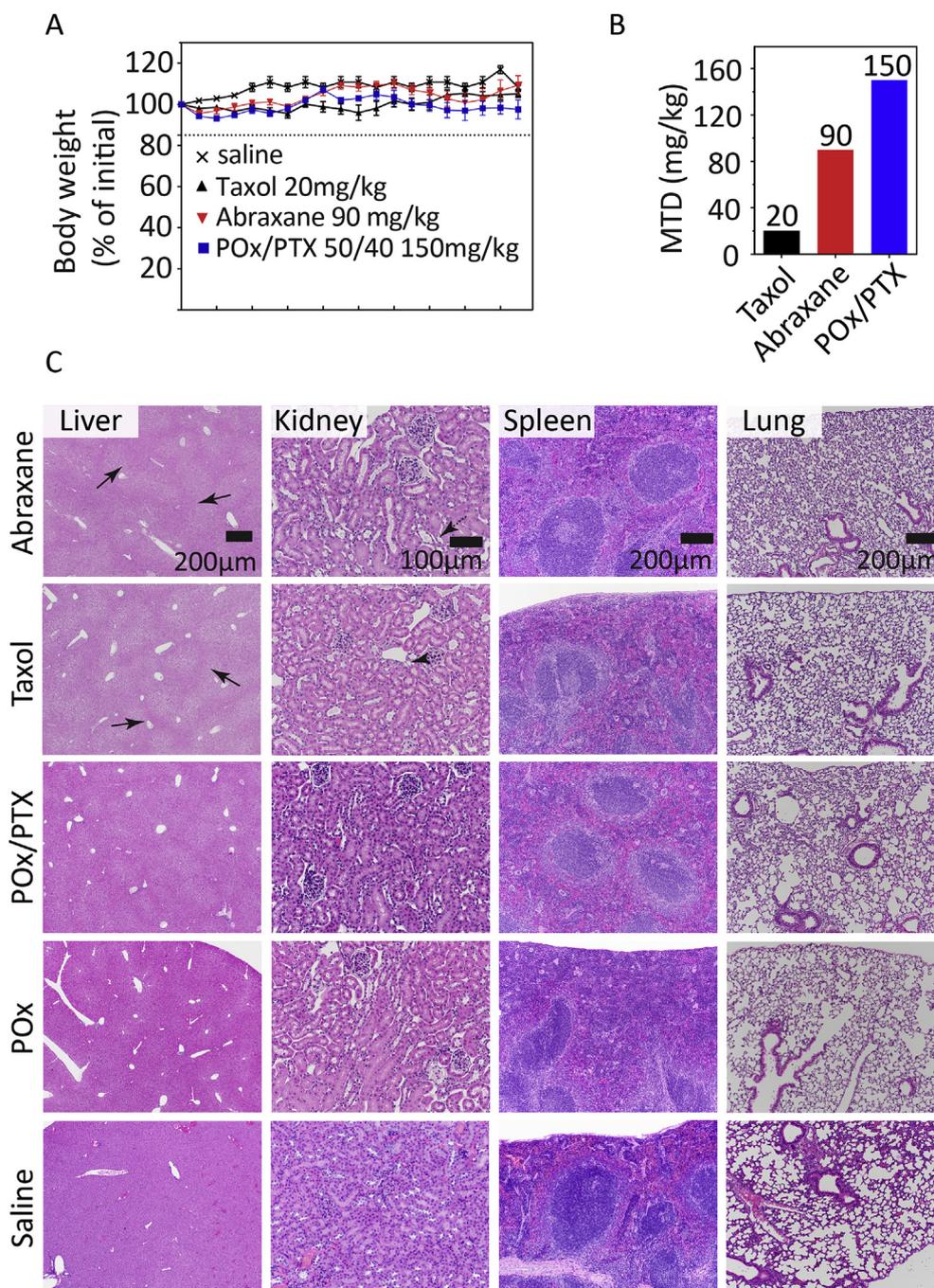
Fig. 4. **MTD in tumor bearing nude mice and toxicology profiles**. (**A**) Mice body weight (% of initial) after repeated administration of various PTX formulations. (**B**) Maximum tolerated dose of the POx/PTX 50/40 formulation (150 mg/kg) is considerably higher as compared to two clinically approved formulations Taxol (20 mg/kg) and Abraxane (90 mg/kg) in a q4d × 4 regimen. (**C**) Histological examination of liver, kidney, spleen, and lung tissues by hemotoxylin & eosin (H&E) staining from animals treated with Abraxane (90 mg PTX/kg), Taxol (20 mg PTX/kg), POx/PTX (50/40, 150 mg/kg), POx (150 mg/kg) or saline. Tissues were harvested two weeks after the last dose of q4d × 4 regimen. Scale bar 200 μm, 100 μm for kidney.

albeit markedly attenuated despite the higher PTX dose. In saline control, this change was absent. Also, Abraxane and Taxol treated animals showed signs of mild toxicity in the kidney with few scattered atrophied tubules with fluid to proteinaceous accumulations to occasional casts (Fig. 4C dashed arrow in kidney samples). Only very little mild and scattered tubular damage was observed in POx/PTX samples (see supplementary information for a more detailed analysis). Overall, our results reinforce the excellent biocompatibility profile of POx reported previously [22–33].

3.4. Drug PK and biodistribution of POx/PTX compared to taxol

The PK and biodistribution profiles of POx/PTX 50/40 and 50/20 micelles at MTD (150 mg/kg) dose in tumor bearing mice (A2780 subcutaneous xenografts) were compared to Taxol 20 mg/kg. PK and biodistribution in tumor-free nude mice are discussed in supplementary information (Fig. S10 and Table S8). It is apparent that when administering Taxol, the PTX concentration in the blood decreases more rapidly [$t_{\frac{1}{2}, \alpha}$ = 2.5 h vs. 3.1 h (50/20) and 3.5 h (50/

40), Table S9]. Also C_{max} of Taxol is approx. one-third of C_{max} of POx/PTX 50/40 and 50/20. The plasma PTX concentration is approx. one order of magnitude higher for the POx/PTX formulations as compared to Taxol formulation (Fig. 5A, Fig. S11A), resulting in much higher tumor drug concentrations (Fig. 5B). Please note, since we injected at MTD, a similar relative dose %ID/g between POx/PTX and Taxol corresponds to approx. 7 times higher values in the absolute dose values (Fig. 5A,B). The peak concentrations in the tumors are reached 1 h p.i. for all investigated formulations, but C_{max} and AUC is considerably higher for both POx/PTX formulations. Similar to plasma concentrations, the intratumoral drug concentration is initially 4—6 fold higher for POx formulations, the difference reaches two orders of magnitudes after 7 days. Overall, the total dose delivered to the tumor ($AUC_{1h-168h}$) is 6—6.5 times higher compared to Taxol control (Table S9). The biodistribution of PTX is very similar for both POx formulations. At early time points, we observed a moderate uptake in spleen, liver, kidney and heart besides tumor uptake. Of all organs, liver exhibited the highest

uptake (%ID/g) after 1 h (Fig. 5C). It must be noted that not only in tumor we found a higher %ID/g as compared to Taxol but also in sensitive tissue, such as the brain. We do not know what the long term effects of this may be, but our results warrant close examination of potential side effects in future preclinical studies.

However, after 24 h and in contrast to Taxol, the tumor-to-organ ratio exceeds unity for all organs examined (Fig. 5D). Injection of the MTD of Taxol slowed down tumor growth and prolonged survival only for approx. 5 days. A single injection of MTD of POx/PTX formulations apparently eradicated the tumors in 4 out of 7 animals, no re-growth was observed up to 28 days after injection (Fig. 5E,F). Although the remaining animals in both groups relapsed starting 7—19 days after administration, survival was significantly prolonged in both cases.

The biodistribution of the polymeric carrier was followed independently by *in vivo* positron emission tomography (PET, Fig. 6 and supplementary videos S1—S8) and tissue sampling after necropsy (Fig. S12) using Cu-64 labeled polymers (see supplementary

▲Taxol 20mg/kg ■ POx/PTX=50/20 150mg/kg ■ POx/PTX=50/40 150mg/kg
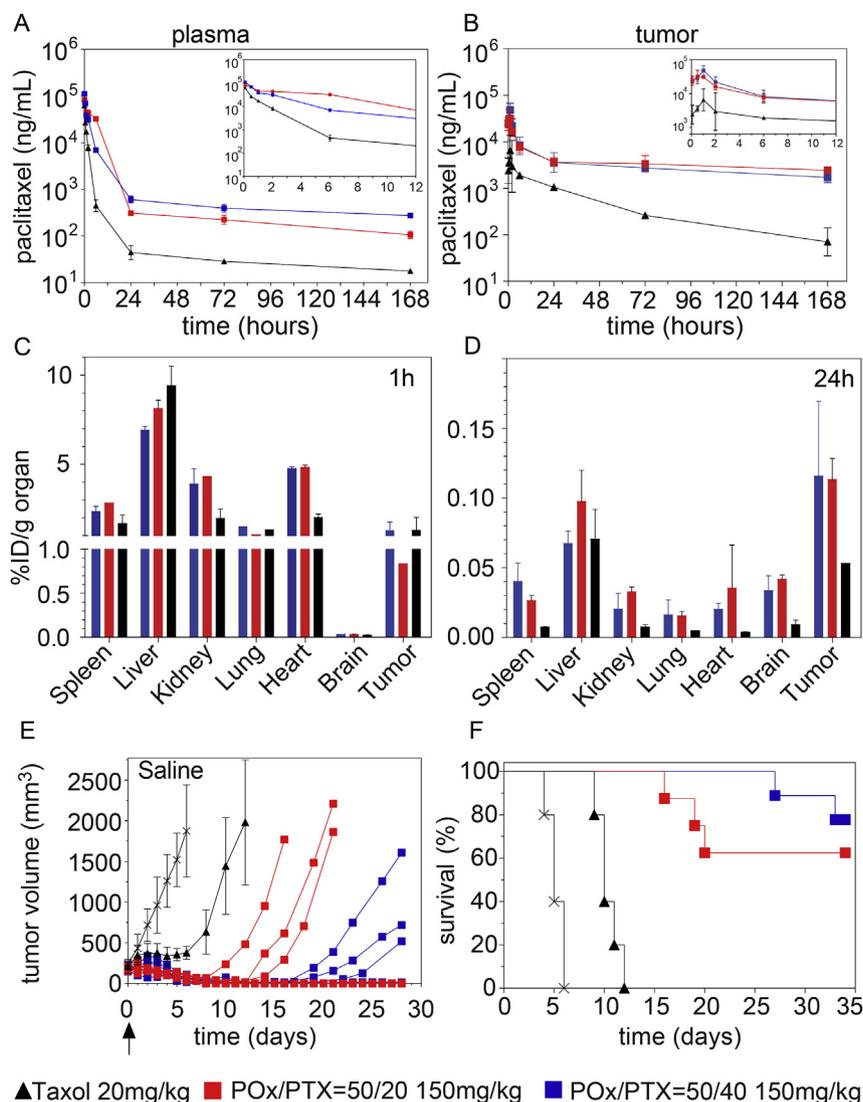
Fig. 5. Pharmacokinetics, biodistribution and tumor inhibition in A2780 human ovarian tumor bearing mice. (**A,B**) Plots of PTX concentration in plasma (**A**) and tumor (**B**) over 168 h following single intravenous (*i.v.*) injection of POx/PTX 50/40 or 50/20 and Taxol formulations at MTD dose. (**C,D**) Biodistribution after single *i.v.* injection of PTX administered as POx/PTX 50/40, POx/PTX 50/20 and Taxol formulation at 1 h p.i. (**C**) and 24 h p.i. (**D**). Tumor growth inhibition (**E**) and Kaplan-Meier survival plots (**F**) of tumor bearing mice after single *i.v.* injection of POx/PTX 50/40, POx/PTX 50/20 and Taxol formulation at MTD. For **A**—**D**, data are expressed as means ± SD, n = 3 for all groups. For **E**, data for Taxol and saline control are expressed as means ± s.e.m., n = 7, while for POx/PTX 50/40, POx/PTX 50/20 nanoformulations, the data of individual animals are presented.

information for a more detailed discussion). As expected, the polymer with a molar mass well below the excretion limit of the kidney (M_n = 10 kg/mol) was readily cleared by the kidney and showed minimal liver uptake, similar to previous observation on small (5 kg/mol) hydrophilic POx [34].

Supplementary video related to this article can be found at http://dx.doi.org/10.1016/j.biomaterials.2016.06.002.

3.5. Antitumor efficacy and tumor accumulation of POx/PTX

After the preliminary experiment using only a single injection, we evaluated antitumor efficacy of POx/PTX in tumor models including A2780 human ovarian cancer xenografts, LCC6-MDR multidrug resistant human triple negative breast cancer (TNBC) orthotopic model and "T11" mouse claudin-low breast cancer model, an orthotopic syngeneic transplants (OST), using a q4d × 4 regimen.

3.5.1. A2780 human ovarian cancer xenografts

We compared treatment at MTD and ½MTD (for POx/PTX and Abraxane) of small (ca. 100–200 mm³) and larger tumors (ca. 400 mm³) to mimic early and late stage disease, respectively. In

small tumors, Taxol delayed tumor growth until the fourth injection after which the lesions started to rapidly grow back (Fig. 7A,C). In contrast, POx/PTX 50/40 exhibited very significant tumor inhibition (p < 0.001). After the third dose, all tumors achieved a complete response. In the Abraxane MTD group, 3 out of 7 mice in Abraxane group experienced severe peripheral neuropathy as evidenced by paralysis and over 15% weight loss that required sacrificing the animals (Fig. 7B,D,E). At ½MTD dose of Abraxane, 40% of mice relapsed after initial tumor shrinkage (Fig. 7B). As a result, survival in the Abraxane regimen was the same for MTD and ½MTD group (Fig. 7D).

For later stage tumors, Taxol did not control tumor (Fig. 8A), while POx/PTX formulations resulted in complete remission of tumors in all animals at MTD and ½MTD even 120 days post treatment (Fig. 8A,B). This remarkable and complete remission was achieved only after four injections of our formulation and in a very aggressive tumor model. The best previous report of complete regression using micellar PTX was done on less aggressive models and required much greater number of injections (from 9 to 11) [35]. Abraxane at MTD also led to complete remission of tumors and survival of all animals, at ½MTD tumors shrunk initially significantly but grew back and survival was significantly lower than in
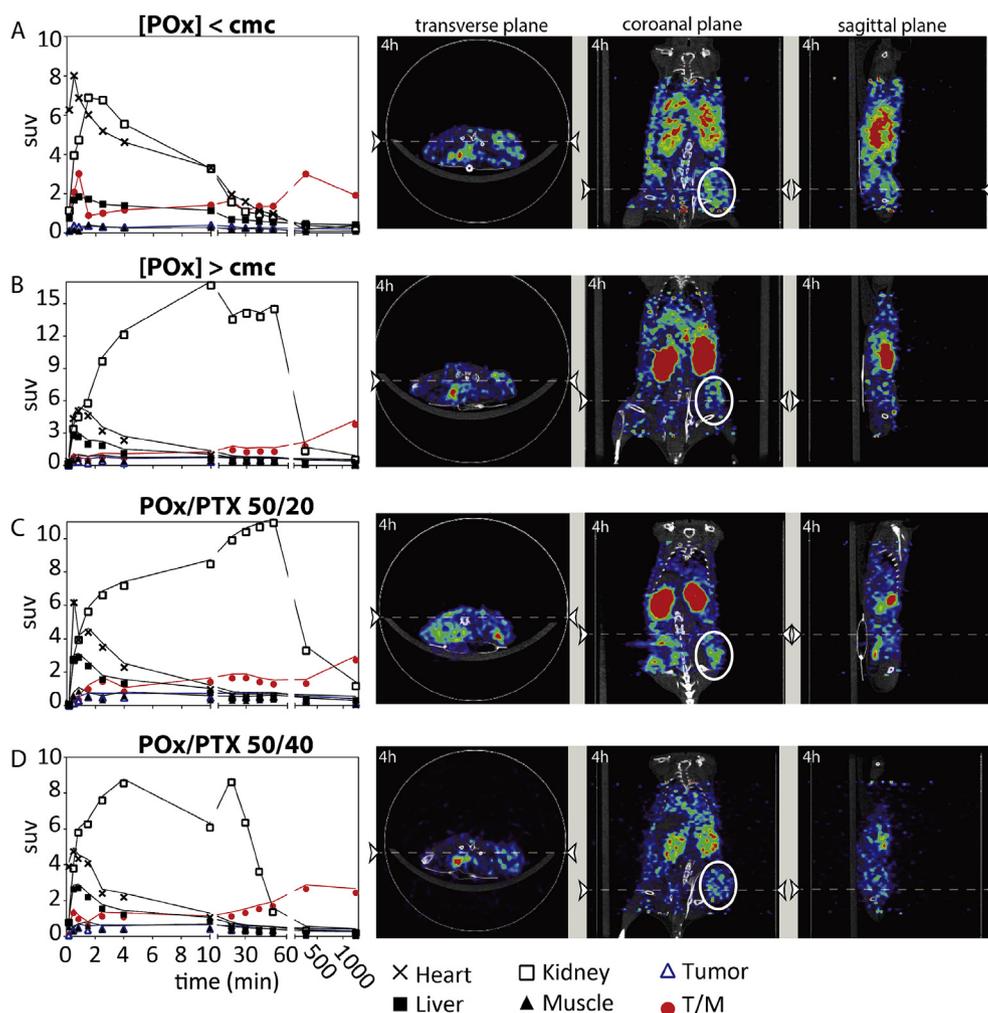
Fig. 6. Tissue biodistribution and PET/CT images of tumor bearing (A2780 xenograft) nude mice obtained after *i.v.* injection of formulations containing 0.2 mCi ^{64}Cu-POx. Mouse injected with (**A**) ^{64}Cu-POx polymer alone below cmc concentration, (**B**) ^{64}Cu-POx 50 micelles without drug loading (at equivalent dose as 50/20), (**C**) ^{64}Cu-POx/PTX 50/20 and (**D**) ^{64}Cu-POx/PTX 50/40 micelle formulation at dose of 150 mg/kg. PET/CT images were taken dynamically for the first hour and then at 4 h and 24 h post *i.v.* injection. Biodistribution data were obtained from quantification of PET images. Strong ^{64}Cu signals were mainly observed in the kidney. Representative PET/CT images were taken at 4 h post injection (n = 1 for each group). Abbreviations: suv-standardized uptake value; T/M-tumor/muscle ratio. Tumor region is circled white.
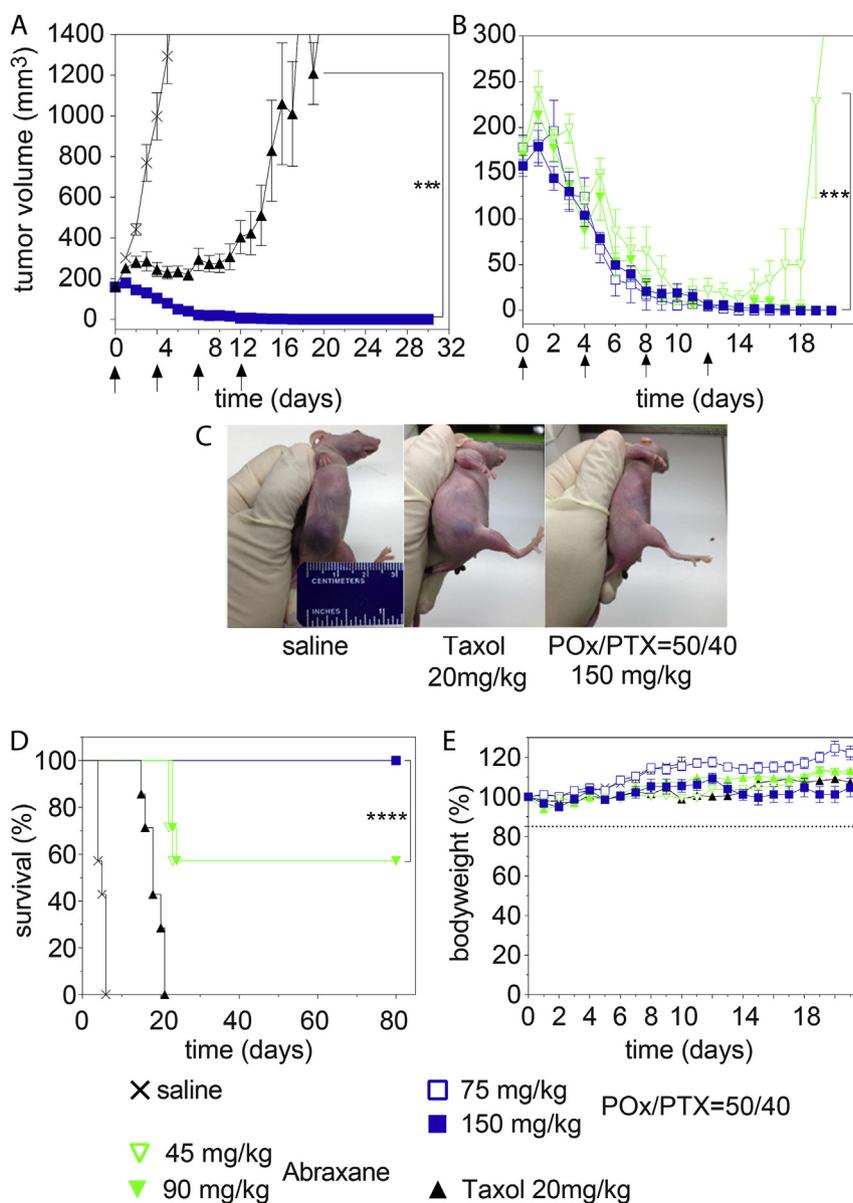
Fig. 7. Antitumor efficacy of PTX formulations in A2780 tumors of small size. a,b, Comparison of tumor growth inhibition of (**A**) POx/PTX 50/40 formulation (@MTD = 150 mg/kg) and Taxol (@MTD = 20 mg/kg), and (**B**) POx/PTX 50/40 formulation (@MTD and ½MTD dose = 150 and 75 mg/kg, respectively) and Abraxane (@MTD and ½MTD = 90 and 45 mg/kg, respectively). Each formulation was injected on days 0, 4, 8, 12. Data is expressed as mean ± s.e.m., n = 7. ***p < 0.001. (**C**) A representative image of mice (day 6) treated with saline (left), Taxol (middle) and POx/PTX 50/40 (right), respectively. (**D**) Kaplan-Meier survival plot for all groups in (**A**) and (**B**) ****p < 0.0001. (**E**) Changes of body weight of animals in each group (mean ± s.e.m., n = 7).

POx/PTX and Abraxane MTD group (Fig. 8B).

3.5.2. Orthotopic model of LCC6-MDR human TNBC [36]

In this model, the previously established MTDs for POx/PTX 50/40 and Abraxane proved to be slightly too high. Thus, experiments were conducted at doses of 80 mg/kg (Abraxane) and 120 mg/kg (POx/PTX). These two treatment groups successfully reduced tumor growth, POx/PTX more so than Abraxane (Fig. 8C). However, Abraxane did not lead to increased survival, while POx/PTX extended survival significantly (Fig. 8D).

3.5.3. T11 OST breast cancer model

This very aggressive tumor model represents a recently identified claudin-low subtype of TNBC with very poor prognosis [37]. This syngeneic transplant model recapitulates clinical tumor types [38], with this particular line being a good mimic of human claudin-

low tumors, and which has been extensively used for treatment studies [39–41].

Several chemotherapeutic agents including carboplatin, PTX, erlotinib and lapatinib were tested in this model as single or two drug combinations but showed no efficacy [39]. The results using the POx/PTX 50/40 formulation in A2780 and LCC6-MDR prompted us to test the POx nanoformulations in the T11 model. We observed clear trend of tumor inhibition in POx/PTX 50/40 ½MTD group and significant suppression at MTD dose (p < 0.01) (Fig. 8E). Furthermore, POx/PTX 50/40 at ½MTD dose also exhibited significant trend (p = 0.016) regarding survival benefit over control groups (Fig. 8F).

4. Discussion

A very simple formulation approach for a clinically established drug results in greatly improved therapeutic outcomes in several of
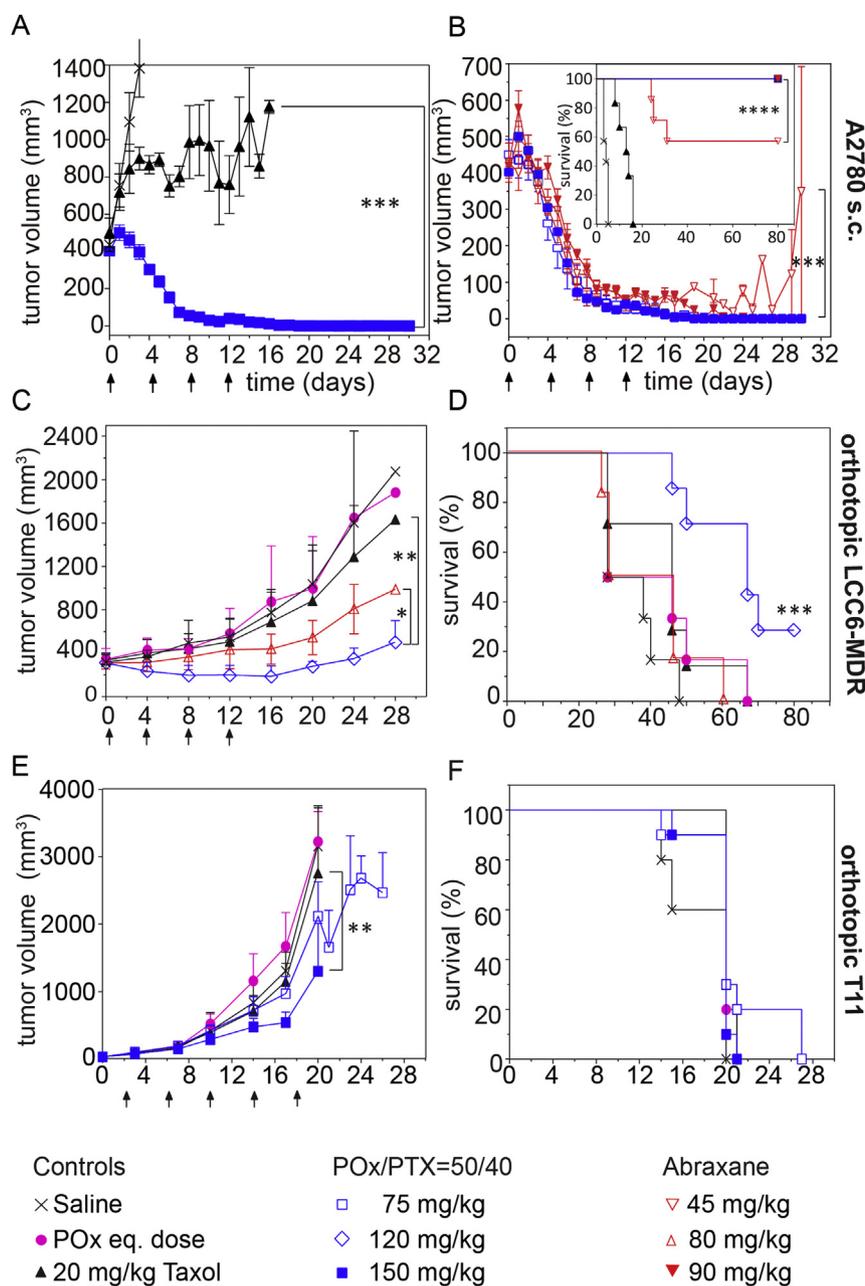
Fig. 8. Antitumor efficacy of various PTX formulations in different tumors. (**A,B**) Comparison of tumor growth inhibition of (**A**) POx/PTX 50/40 formulation (@MTD dose = 150 mg/kg) and Taxol (@MTD dose = 20 mg/kg), and (**B**) POx/PTX 50/40 formulation (@MTD and ½MTD dose = 150 and 75 mg/kg, respectively) compared to Abraxane (@MTD and ½MTD dose = 90 and 45 mg/kg). Growth inhibition in triple negative breast cancer (**C**) and survival (**D**) of mice bearing LCC6-MDR tumors. Treatment was performed at respective MTDs or dose of polymer corresponding to MTD (POx control). (**E,F**) Tumor growth inhibition (**E**) and survival (**F**) of mice bearing T11 tumors. Treatment was performed at respective MTD and ½MTD dose or dose of polymer corresponding to MTD (POx control). The formulation was injected on days (**A—D**) 0, 4, 8, and 12, or (**E,F**) 2, 6, 10, 14, and 18, respectively. Data is expressed as mean ± s.e.m., n = 7. *$p < 0.05$, **$p < 0.01$, ***$p < 0.001$.

tumor models compared to clinically applied formulations. This shows promise for further development of novel excipients employing amphiphilic polymers. The POx/PTX nanoformulations feature a controllable and defined size (20—80 nm, PDI ~ 0.1), which is particularly desirable for systemic drug delivery. Small angle neutron scattering data suggest formation of amorphous nanoparticles with hydrodynamic radii <50 nm [16]. Nanoparticles in this size range are believed to be particularly useful in cancer chemotherapy because such small sized entities exhibit superior penetration in poorly permeable tumors [42]. However, considering our results on serum stability and relatively short circulation

time of our formulation, in this particular case we would not expect a major contribution of the "enhanced permeability and retention" (EPR) effect.

Notably, the polymer design proved to be of major importance in our studies. The hydrophilic block is poly(2-methyl-2-oxazoline) (PMeOx), which imposes stealth properties similar if not superior to PEG [43,44]. The hydrophobic block, poly(2-butyl-2-oxazoline) (PBuOx) was screened as an ideal environment for solubilizing unprecedentedly high amount of PTX with outstanding formulation stability [14,15,45]. Moreover, triblock structure proved superior as compared to diblock structure [11]. In this environment even

at very high loading the drug remains molecularly dispersed in the micelle having a raspberry-like morphology [16]. We have followed some batches of nanoformulations for months and observed no changes at ambient conditions [16]. Due to their low viscosity, they can be readily injected as prepared at high concentration. Such formulation properties compare very favorably to other PTX formulations in clinics and in late stage clinical trials. At maximum loading (POx/PTX 50/45 g/L), the drug release *in vitro* appears to be slightly faster as compared to lower loading (POx/PTX 50/40 g/L) (Fig. S3). The basic characteristics such as relative and absolute PTX concentration of the POx/PTX formulation compares very favorably to the only currently FDA approved PTX formulations Taxol and Abraxane as well as other PTX formulations currently in advanced clinical trials such as NK105 and Genexol-PM. Especially striking is the difference of PTX concentration in the injected form, in which both these polymer amphiphile formulations comprise less then 1 g/L paclitaxel concentration (0.12 g/L and 0.6 g/L for NK105 and Genexol-PM, respectively), while POx/PTX can be injected at 40 g/L.

The unparalleled high drug loading and drug concentration achieved with the POx micelle formulation enable a significant decrease of the excipient dose and injection volume (>60 and >300 fold lower volume for same PTX dose compared to Genexol-PM and NK105, respectively). This may be a factor for the extraordinary high MTD as compared to Taxol and Abraxane. Due to the favorable safety profile, we hypothesize that the POx/PTX formulations may result in clinically relevant advantages over current approved formulations, allowing a high dose of PTX to be given to maximize the therapeutic effect.

Although the POx/PTX formulations are stable for months in solution [16], we cannot assume *a priori* that they are also stable in the presence of high protein concentrations and other potential "sinks" as the blood. We chose a label-free approach, and investigated the quenching of albumin tryptophan fluorescence in the presence of polymer and POx/PTX formulations. In brief, two important results were obtained. First, the polymer alone leads to minor but noticeable concentration dependent fluorescence quenching, indicative of weak polymer-protein interactions. Second, drug formulations produced a more pronounced concentration-dependent fluorescence quenching. The quenching was dependent on the polymer content in the formulation — the higher polymer content decreased the fluorescence quenching, which we attribute to competition of the micelles with the serum protein for the drug binding. More detailed studies, including fluorescence lifetime measurements are warranted, but we conclude from these results that serum albumin represents a sink for PTX from POx/PTX formulations and that there is a rapid exchange between the two PTX loci. For the *in vivo* situation, we envision that the PTX can be released from the micelles to serum albumin to reach a highly dynamic equilibrium as the polymer unimers are excreted via the kidneys. However, it should be noted that compared Taxol that is known to rapidly release PTX in serum [5], the POx/PTX formulations are more stable in the presence of serum as follows from our SPE column experiment. Moreover, as the POx/PTX dose increases to 150 mg/kg the amount of the drug associated with the micellar fraction also increases to over 80% possibly due to the saturation of the PTX binding sites in the serum proteins. Therefore, at least in the initial moment when concentration of the POx/PTX in the blood is very high (estimated 2.5 mM PTX compared to ~0.5 mM serum protein [5]) a significant portion of the administered drug may still remain in the micelles. This may help explaining the fact that the MTD in the case of our formulations is much higher than that of Abraxane. The high value we found for protein bound paclitaxel in the case of Taxol is in line with well-known high protein bound fraction of approx. 92%–97% in humans [5]. Therefore, it is reasonable to assume that compared to Taxol formulation POx

micelles have much better retention of PTX and are more stable in the presence of the serum. Moreover, as the ratio of the drug in POx/PTX formulation increases the fraction of the drug associated with the POx micelles also increases.

The biodistribution of radiolabeled polymer indicates that the amphiphilic POx has a similarly favorable biodistribution as the purely hydrophilic POx does. The very low liver uptake of the polymer observed may prove to be beneficial in repeated treatment regimens. The PK data of drug-loaded polymeric micelles show a strongly elevated drug exposure to tumor tissues and consequently an enhanced antitumor activity with significantly prolonged survival.

The benefit in survival in A2780 and LCC6-MDR models over both Taxol and Abraxane is remarkable and is very promising for further development. In the case of A2780 we investigated tumor growth inhibition and survival for small and large tumor models. In both cases, we found that in contrast to Taxol and Abraxane, the tumors were apparently completely eradicated in all animals at MTD and ½ MTD (no regrowth after treatment regimen up to day 80 after treatment initiation) (Fig. 7 and 8A,B). This lead to a drastic increase in the animal survival (Figs. 7D and 8B insert). In the multidrug resistant LCC6-MDR model, tumors were not eradicated but shrank initially during treatment, which was not observed in the Taxol and Abraxane groups. While Taxol led to no appreciable delay in the tumor growth, Abraxane slowed it down significantly (Fig. 8C). However, no survival benefit was observed for both clinically approved formulations, in contrast to the group treated with POx/PTX formulation (Fig. 8D). It appears that the increased MTD observed for the POx/PTX formulation correlates with increased antitumor efficacy. The PK studies showed that over the course of 7 days, approx. 6 times more drug reached the tumor (Table S9). Obviously, one can expect a higher antitumor efficacy if more drug is administered and delivered to the tumor. In this regard POx/PTX micelle formulation may have a clear advantage over both Taxol and Abraxane. However, possible long-term effects of high drug doses on other organs will have to be assessed further in more detailed toxicity studies that are outside the scope of this work. A direct comparison to the two polymeric formulations NK105 and Genexol-PM currently in clinical trials was not possible at this point. However, one can compare some key features of the PK studies in mice available for both formulations. Kim et al. compared PK of PTX after administration of Taxol (20 mg/kg) and Genexol-PM (50 mg/kg) in mice bearing B16 melanoma [11]. Time of maximal concentration of the drug in the tumor was early after administration for both formulations (1 h for Genexol-PM and 2 h for Taxol, respectively). Therefore, Genexol-PM apparently does not exhibit the prolonged circulation one might expect from a PEGylated nanoparticle. Interestingly, $AUC_{0-\infty}$ and C_{max} was reportedly higher for Taxol than for Genexol-PM despite the higher injected dose. In contrast, in the present case of POx/PTX, the AUC and C_{max} correlate well with the injected dose. Despite the seemingly unfavorable PK parameters, Genexol-PM performed well with respect to antitumor efficacy, where it outperformed Taxol in a SKOV-3 human ovarian tumor xenograft and a MX-1 human breast cancer xenograft. In contrast to the situation for Genexol-PM and POx/PTX, there is clear experimental evidence of prolonged circulation of PTX in the case of NK105 [12]. Times of maximal drug concentration in the tumor was up to 24 h. Also, $AUC_{0-\infty}$ was more than 20 times higher for NK105 as compared to PTX alone. Accordingly, also NK105 clearly outperformed Taxol with respect to antitumor efficacy in the chosen model (HT-29) with tumors apparently eradicated in all animals at MTD. However, it should be noted that at ½ MTD, some tumors clearly grew back and follow-up time was rather short (<35 days). It should be also noted that it remains somewhat unclear in what form the control PTX was injected in this work.

Also in the T11 model a significant trend of extension in survival was observed. However, there was only a trend towards positive therapeutic outcome in this very challenging model. Although our results comparing the performance of PTX/POx micelle formulations with Taxol and Abraxane are striking, we would like to point out that the latter two formulations of the PTX were evaluated in numerous clinical trials and have been commercially available. Therefore, the true potential of PTX/POx micelle needs to be evaluated based of the extensive further pre-clinical and clinical evaluation. It should be noted that the amphiphilic POx was previously implemented in the formulation of various multiple drug combinations, some of which have shown synergy with PTX *in vitro* [15]. Therefore, we hypothesize that treatment with multiple drugs co-loaded in POx micelles may be beneficial in this very challenging model.

Overall, we present here promising preclinical data on POx/PTX nanoformulation that provide a robust rationale for further development. Increased safety along with a high drug dose treatment may ultimately benefit patient survival and quality-of-life, which is not provided by Abraxane in comparison to Taxol.

Author Contributions

A.S. and H.B. synthesized and analyzed polymers, R.L. and R.J. supervised synthesis and characterization. Z.H. and X.W. performed fluorescence quenching experiments, X.W., R.L. and A.V.K. analyzed and interpreted the data. X.W. performed serum binding studies, X.W., A.V.K and R.L analyzed the data. Z.H., X.W. and A.S. performed formulation and *in vitro* release experiments. Z.H. and X.W. performed *in vivo* animal studies of POx/PTX formulation and analyzed experimental data. D.B.D. and C.M.P. supervised tumor model studies. D.Y.A., and M.S., reviewed primary data and figures, and participated in animal studies experiment design. M.A.D. and S.T.S. designed, conducted and analyzed cytotoxicity, complement activation and hemocompatibility experiments. S.A.M. performed histological analysis. H.Y., Z.L., and Z.H. designed and performed the Cu64 labeling and PET imaging experiments and analyzed the data. Z.H., R.L. and A.V.K. wrote the manuscript. R.L., R.J. and A.V.K. supervised and designed the entire study.

Acknowledgments

Appendix A. Supplementary data

Supplementary data related to this article can be found at http://dx.doi.org/10.1016/j.biomaterials.2016.06.002.

References

[1] M.C. Wani, H.L. Taylor, M.E. Wall, P. Coggon, A.T. McPhail, Plant antitumor Agents.VI. Isolation and structure of taxol, a novel antileukemic and antitumor agent from Taxus brevifolia, J. Am. Chem. Soc. 93 (1971) 2325—2327.

[2] Z. Zhang, L. Mei, S.-S. Feng, Paclitaxel drug delivery systems, Expert Opin. Drug. Deliv. 10 (2013) 325—340.

[3] L.M. Zasadil, K.A. Andersen, D. Yeum, G.B. Rocque, L.G. Wilke, A.J. Tevaarwerk, R.T. Raines, M.E. Burkard, B.A. Weaver, Cytotoxicity of paclitaxel in breast cancer is due to chromosome missegregation on multipolar spindles, Sci. Transl. Med. 6 (2014) 229ra43.

[4] R.T. Liggins, W.L. Hunter, H.M. Burt, Solid-state characterization of paclitaxel, J. Pharm. Sci. 86 (1997) 1458—1463.

[5] E. Brouwer, J. Verweij, P. De Bruijn, W.J. Loos, M. Pillay, D. Buijs, A. Sparreboom, Measurement of fraction unbound paclitaxel in human plasma, Drug Metab. Disp. 28 (2000) 1141—1145.

[6] R.B. Weiss, R.C. Donehower, P.H. Wiernik, T. Ohnuma, R.J. Gralla, D.L. Trump, J.R. Baker, D.A. Van Echo, D.D. Von Hoff, B. Leyland-Jones, Hypersensitivity reactions from taxol, J. Clin. Oncol. 8 (1990) 1263—1268.

[7] A. Sparreboom, O. van Tellingen, W.J. Nooijen, J.H. Beijnen, Nonlinear pharmacokinetics of paclitaxel in mice results from the pharmaceutical vehicle cremophor EL, Cancer Res. 56 (1996) 2112—2115.

[8] Y. Yamamoto, I. Kawano, H. Iwase, Nab-paclitaxel for the treatment of breast cancer: efficacy, safety, and approval, Onco. Targets Ther. 4 (2011) 123.

[9] A. Sparreboom, C.D. Scripture, V. Trieu, P.J. Williams, T. De, A. Yang, B. Beals, W.D. Figg, M. Hawkins, N. Desai, Comparative preclinical and clinical pharmacokinetics of a cremophor-free, nanoparticle albumin-bound paclitaxel (ABI-007) and paclitaxel formulated in cremophor (taxol), Clin. Cancer Res. 11 (2005) 4136—4143.

[10] H.S. Rugo, W.T. Barry, A. Moreno-Aspitia, A.P. Lyss, C. Cirrincione, E.L. Mayer, M. Naughton, R.M. Layman, L.A. Carey, R.A. Somer, in: ASCO Annual Meeting Proceedings, vol. 30, 2012, p. CRA1002.

[11] S.C. Kim, D.W. Kim, Y.H. Shim, J.S. Bang, H.S. Oh, S.W. Kim, M.H. Seo, In vivo evaluation of polymeric micellar paclitaxel formulation: toxicity and efficacy, J. Control. Release 72 (2001) 191—202.

[12] T. Hamaguchi, Y. Matsumura, M. Suzuki, K. Shimizu, R. Goda, I. Nakamura, I. Nakatomi, M. Yokoyama, K. Kataoka, T. Kakizoe, NK105, a paclitaxel-incorporating micellar nanoparticle formulation, can extend in vivo anti-tumour activity and reduce the neurotoxicity of paclitaxel, Br. J. Cancer 92 (2005) 1240—1246.

[13] K. Kato, K. Chin, T. Yoshikawa, K. Yamaguchi, Y. Tsuji, T. Esaki, K. Sakai, M. Kimura, T. Hamaguchi, Y. Shimada, et al., Phase II study of NK105, a paclitaxel-incorporating micellar nanoparticle, for previously treated advanced or recurrent gastric Cancer, Investig. New Drugs 30 (2012) 1621—1627.

[14] R. Luxenhofer, A. Schulz, C. Roques, S. Li, T.K. Bronich, E.V. Batrakova, R. Jordan, A.V. Kabanov, Doubly amphiphilic poly(2-oxazoline)s as high-capacity delivery systems for hydrophobic drugs, Biomaterials 31 (2010) 4972—4979.

[15] Y. Han, Z. He, A. Schulz, T.K. Bronich, R. Jordan, R. Luxenhofer, A.V. Kabanov, Synergistic combinations of multiple chemotherapeutic agents in high capacity poly(2-oxazoline) micelles, Mol. Pharm. 9 (2012) 2302—2313.

[16] A. Schulz, S. Jaksch, R. Schubel, E. Wegener, Z. Di, Y. Han, A. Meister, J. Kressler, A.V. Kabanov, R. Luxenhofer, C.M. Papadakis, R. Jordan, Drug-induced morphology switch in drug delivery systems based on poly(2-oxazoline)s, ACS Nano 8 (2014) 2686—2696.

[17] J. Khandare, A. Mohr, M. Calderon, P. Welker, K. Licha, R. Haag, Structure biocompatibility relationship of dendritic polyglycerol derivatives, Biomaterials 31 (2010) 4268—4277.

[18] M. Senthil, P. Chaudhary, D.D. Smith, P.E. Ventura, P.H. Frankel, V. Pullarkat, V. Trisal, A shortened activated partial thromboplastin time predicts the risk of catheter-associated venous thrombosis in cancer patients, Thromb. Res. 134 (2014) 165—168.

[19] T. Hamaguchi, K. Kato, H. Yasui, C. Morizane, M. Ikeda, H. Ueno, K. Muro, Y. Yamada, T. Okusaka, K. Shirao, et al., A phase I and pharmacokinetic study of NK105, a paclitaxel-incorporating micellar nanoparticle formulation, Br. J. Cancer 97 (2007) 170—176.

[20] M.J. Hawkins, P. Soon-Shiong, N. Desai, Protein nanoparticles as drug carriers in clinical medicine, Adv. Drug. Deliv. Rev. 60 (2008) 876—885.

[21] K.S. Lee, H.C. Chung, S.A. Im, Y.H. Park, C.S. Kim, S.B. Kim, S.Y. Rha, M.Y. Lee, J. Ro, Multicenter phase II trial of genexol-PM, a cremophor-free, polymeric micelle formulation of paclitaxel, in patients with metastatic breast cancer, Breast Cancer Res. Treat. 108 (2008) 241—250.

[22] R. Luxenhofer, G. Sahay, A. Schulz, D. Alakhova, T.K. Bronich, R. Jordan, A.V. Kabanov, Structure-property relationship in cytotoxicity and cell uptake of poly(2-oxazoline) amphiphiles, J. Control. Release 153 (2011) 73—82.

[23] R. Luxenhofer, Y. Han, A. Schulz, J. Tong, Z. He, A.V. Kabanov, R. Jordan, Poly(2-oxazoline)s as polymer therapeutics, Macromol. Rapid Commun. 33 (2012) 1613—1631.

[24] N. Zhang, T. Pompe, I. Amin, R. Luxenhofer, C. Werner, R. Jordan, Tailored polymer brushes of poly(2-oxazoline)s to control the protein adsorption and cell adhesion, Macromol. Biosci. 7 (2012) 926—936.

[25] J. Tong, X. Yi, R. Luxenhofer, W.A. Banks, R. Jordan, M.C. Zimmerman, A.V. Kabanov, Conjugates of superoxide dismutase 1 with amphiphilic poly(2-oxazoline) block copolymers for enhanced brain delivery: synthesis,

characterization and evaluation in vitro and in vivo, Mol. Pharm. 10 (2013) 360—377.

[26] D.L. Kyluik-Price, L. Li, M.D. Scott, Comparative efficacy of blood cell immunocamouflage by membrane grafting of methoxypoly(ethylene glycol) and polyethyloxazoline, Biomaterials 35 (2014) 412—422.

[27] K.L. Eskow Jaunarajs, D.G. Standaert, T.X. Viegas, M.D. Bentley, Z. Fang, B. Dizman, K. Yoon, R. Weimer, P. Ravenscroft, T.H. Johnston, et al., Rotigotine polyoxazoline conjugate SER-214 provides robust and sustained anti-parkinsonian benefit, Mov. Disord. 28 (2013) 1675—1682.

[28] M. Bauer, S. Schroeder, L. Tauhardt, K. Kempe, U.S. Schubert, D. Fischer, In vitro hemocompatibility and cytotoxicity study of poly (2-methyl-2-oxazoline) for biomedical applications, J. Polym. Sci. Part A Polym. Chem. 51 (2013) 1816—1821.

[29] J. Ulbricht, R. Jordan, R. Luxenhofer, On the biodegradability of polyethylene glycol, polypeptoids and poly(2-oxazoline)s, Biomaterials 35 (2014) 4848—4861.

[30] Z. He, L. Miao, R. Jordan, D. S-Manickam, R. Luxenhofer, A.V. Kabanov, A low protein binding cationic poly(2-oxazoline) as non-viral vector, Macromol. Biosci. 15 (2015) 1004—1020.

[31] Y. Chen, B. Pidhatika, T. von Erlach, R. Konradi, M. Textor, H. Hall, T. Lühmann, Comparative assessment of the stability of nonfouling poly(2-methyl-2-oxazoline) and poly(ethylene glycol) surface films: an in vitro cell culture study, Biointerphases 9 (2014) 031003.

[32] Z. He, A. Schulz, X. Wan, J. Seitz, H. Bludau, D.Y. Alakhova, D.B. Darr, C.M. Perou, R. Jordan, I. Ojima, et al., Poly(2-oxazoline) based micelles with high capacity for 3rd generation taxoids: preparation, in vitro and in vivo evaluation, J. Control. Release 208 (2015) 67—75.

[33] P.H. Kierstead, H. Okochi, V.J. Venditto, T.C. Chuong, S. Kivimae, J.M. Fréchet, F.C. Szoka, The effect of polymer backbone chemistry on the induction of the accelerated blood clearance in polymer modified liposomes, J. Control. Release 213 (2015) 1—9.

[34] F.C. Gaertner, R. Luxenhofer, B. Blechert, R. Jordan, M. Essler, Synthesis, biodistribution and excretion of radiolabeled poly(2-alkyl-2-oxazoline)s, J. Control. Release 119 (2007) 291—300.

[35] Y. Shi, R. van der Meel, B. Theek, E. Oude Blenke, E.H. Pieters, M.H. Fens, J. Ehling, R.M. Schiffelers, G. Storm, C.F. van Nostrum, et al., Complete regression of xenograft tumors upon targeted delivery of paclitaxel via Π-Π stacking stabilized polymeric micelles, ACS Nano 9 (2015) 3740—3752.

[36] F. Leonessa, D. Green, T. Licht, A. Wright, K. Wingate-Legette, J. Lippman, M.M. Gottesman, R. Clarke, MDA435/LCC6 and MDA435/LCC6MDR1: ascites models of human breast Cancer, Br. J. Cancer 73 (1996) 154—161.

[37] A. Prat, J.S. Parker, O. Karginova, C. Fan, C. Livasy, J.I. Herschkowitz, X. He, C.M. Perou, Phenotypic and molecular characterization of the claudin-low intrinsic subtype of breast cancer, Breast Cancer Res. 12 (2010) R68.

[38] J.I. Herschkowitz, W. Zhao, M. Zhang, J. Usary, G. Murrow, D. Edwards, J. Knezevic, S.B. Greene, D. Darr, M.A. Troester, et al., Comparative oncogenomics identifies breast tumors enriched in functional tumor-initiating cells, Proc. Natl. Acad. Sci. U. S. A. 109 (2012) 2778—2783.

[39] J. Usary, W. Zhao, D. Darr, P.J. Roberts, M. Liu, L. Balletta, O. Karginova, J. Jordan, A. Combest, A. Bridges, Predicting drug responsiveness in human cancers using genetically engineered mice, Clin. Cancer. Res. 19 (2013) 4889—4899.

[40] V.D. Haakensen, O.C. Lingjærde, T. Lüders, M. Riis, A. Prat, M.A. Troester, M.M. Holmen, J.O. Frantzen, L. Romundstad, D. Navjord, Gene expression profiles of breast biopsies from healthy women identify a group with claudin-low features, BMC Med. Genom. 4 (2011) 77.

[41] G. Song, D.B. Darr, C.M. Santos, M. Ross, A. Valdivia, J.L. Jordan, B.R. Midkiff, S. Cohen, N. Nikolaishvili-Feinberg, C.R. Miller, et al., Effects of tumor micro-environment heterogeneity on nanoparticle disposition and efficacy in breast Cancer tumor models, Clin. Cancer. Res. 20 (2014) 6083—6095.

[42] H. Cabral, Y. Matsumoto, K. Mizuno, Q. Chen, M. Murakami, M. Kimura, Y. Terada, M.R. Kano, K. Miyazono, M. Uesaka, et al., Accumulation of sub-100 nm Polymeric micelles in poorly permeable tumours depends on size, Nat. Nanotechnol. 6 (2011) 815—823.

[43] M.C. Woodle, C.M. Engbers, S. Zalipsky, New amphipatic polymer-lipid conjugates forming long-circulating reticuloendothelial system-evading liposomes, Bioconjug. Chem. 5 (1994) 493—496.

[44] T.X. Viegas, M.D. Bentley, J.M. Harris, Z. Fang, K. Yoon, B. Dizman, R. Weimer, A. Mero, G. Pasut, F.M. Veronese, Polyoxazoline: chemistry, properties, and applications in drug delivery, Bioconjug. Chem. 22 (2011) 976—986.

[45] Y. Seo, A. Schulz, Z. Han, H. Bludau, X. Wan, J. Tong, T.K. Bronich, R. Luxenhofer, R. Jordan, A.V. Kabanov, Poly(2-oxazoline) block copolymer based formulations of taxanes: effect of copolymer and drug structure, concentration and environmental factors, Polym. Adv. Technol. 26 (2015) 837—850.